Multiple Solutions in Electrostatic MEMS

J.A. Pelesko*

* Georgia Institute of Technology, School of Mathematics
Atlanta, GA, 30332-0160, pelesko@math.gatech.edu

ABSTRACT

The pull-in voltage instability is the principle phenomena limiting the design of nearly every electrostatically actuated MEMS device. In this instability, when applied voltages are increased beyond a certain critical voltage there is no longer a steady state configuration of the device where mechanical members remain separate. Mathematically, this phenomena has always been explained by the presence of a single fold in the bifurcation diagram for the system. Here a generalized model of a small aspect ratio electrostatically actuated MEMS device is presented. The small aspect ratio assumption permits reduction of the model to a nonlinear partial differential equation describing device deflection. Variations in the electric field due to varying dielectric properties or varying electrode placement are included in the model. By examining several special cases it is shown that the bifurcation diagram for such a device may be much richer than previously supposed.

Keywords: electrostatic actuation, pull-in, instability, semilinear elliptic problem

1 Introduction

The pull-in voltage instability is a universal phenomena in the world of electrostatically actuated MEMS devices. Even as early as 1967, MEMS pioneers such as Nathanson, [1], were aware that when applied voltages are increased beyond a certain critical voltage there is no longer a steady state configuration of the device where mechanical members remain separate.

Mathematically, this instability has always been explained by the presence of a single fold in the bifurcation diagram for the system. That is, when some norm of the solution is plotted versus the applied voltage, a plot similar to Figure 1 is obtained. This bifurcation diagram was originally obtained by Nathanson et.al., [1], in their analysis of a mass-spring model. Subsequently, it has been reproduced by numerous authors through analysis of mass-spring models, [2], experiment, [2], analysis of membrane or beam models, [3]–[6] or as the result of numerical simulation, [7], [8].

The key feature of the bifurcation diagram shown in Figure 1 is that for a given applied voltage precisely zero,

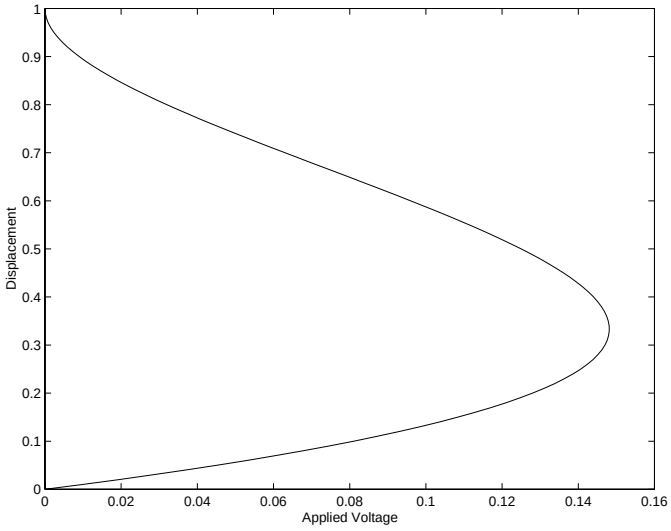

Figure 1: The standard bifurcation diagram for an electrostatically actuated MEMS device.

one or two steady state solutions exist for the electrostatically actuated device being studied. In this paper we show that the situation may be considerably more complicated. That is, the bifurcation diagram may be much richer than the one shown in Figure 1. We begin by presenting a mathematical model of an idealized device. We assume the device is of small aspect ratio so that fringing fields may be ignored and a simplified solution for the electrostatic potential obtained. We use this potential in a membrane based model for the deflection of the device. Our model accounts for varying dielectric properties of the device or varying electrode placement. We summarize the analysis of the model for three key cases: a perfectly conducting strip, a perfectly conducting disk and a strip with varying dielectric properties. We show that in the first case the bifurcation diagram appears as in Figure 1 while in the second and third cases it appears as in Figure 3.

2 The Mathematical Model

In this section we present the governing equations for the behavior of an idealized electrostatically actuated MEMS device. The geometry of the device is sketched

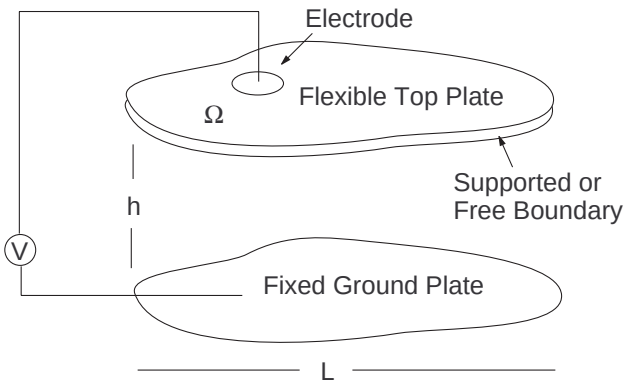

Figure 2: A Sketch of the Model Geometry.

in Figure 2. We assume that a potential difference is applied between the top and bottom plates. The top plate may be a perfect conductor, a dielectric material or may have spatially varying dielectric properties. The electrode attached to the top plate may occupy all or only a portion of the region Ω. Our goal is to formulate a model which captures the steady state deflection of the top plate as a function of the applied voltage.

The mathematical model consists of two parts. First, we need to compute the electrostatic potential everywhere between, on and when the plates are treated as finite thickness dielectric slabs, within the two plates. In general, this requires solving Laplace's equation in the region between and inside the plates with the appropriate applied potential and continuity boundary conditions. Given that the deformation of the top plate is unknown a priori and that the shape of the domain Ω may be quite complicated this problem generally prohibits an exact solution. On the other hand, many MEMS devices posses a small aspect ratio. That is $h/L \ll 1$. This fact can be used to develop an asymptotic approximation to the potential fields in the limit of small aspect ratio. In engineering parlance, fringing fields may be ignored. Space prevents us from providing details, the interested reader is directed to [4]–[6]. Here, we simply note that the electrostatic force, F_e, on the top plate is well approximated by

$$F_e = \frac{\epsilon_0 V^2}{2h^2} \frac{f(x,y)}{(1+u(x,y))^2}. \tag{1}$$

Here, V is the applied potential difference, ϵ_0 is the permitivity of free space and h is the distance between the plates when no voltage difference is applied. The function $f(x,y)$ captures spatial dependence of the applied field due to varying electrode placement or varying dielectric properties. If the top plate is a perfect conductor and the electrode region is all of Ω, then $f(x,y) = 1$. The function $u(x,y)$ is the displacement of the top plate scaled by h.

Next, we need to compute the deflection, $u(x,y)$, of the top plate. The appropriate elastic model depends on the device one wishes to consider. Due to the plethora of MEMS devices, no one model will be appropriate in all situations. Here, we restrict our attention to devices, such as the GLV, [9], which may be treated as elastic membranes. Hence, the deflection of the top plate satisfies the semi-linear elliptic equation

$$\nabla^2 u = \frac{\lambda f(x,y)}{(1+u)^2} \quad \text{in} \quad \Omega. \tag{2}$$

Here $\lambda = V^2 \epsilon_0 L^2 / 2Th^2$ where T is the tension in the membrane and L is a characteristic length of the region Ω. Equation (2) must be supplemented by the appropriate boundary conditions. In general, these may be written in terms of a boundary operator B, that is we require

$$Bu = 0 \quad \text{on} \quad \partial\Omega. \tag{3}$$

A complete analysis of equations (2)-(3) is daunting. Some general results are however possible. For example, it is shown in [12] that for physically realistic choices of $f(x,y)$ the pull-in instability always exists. The reader is referred to [12] for more details and further general results. Here, we focus on analyzing the model for several simple choices of geometry in order to illustrate the range of possible behaviors.

3 A Strip Shaped Domain

If the domain Ω is assumed to be a rectangular strip with two opposite edges fixed and the remaining two edges free, the displacement may be assumed a function of x only. In this case, equations (2-3) reduce to

$$\frac{d^2u}{dx^2} = \frac{\lambda}{(1+u)^2} \tag{4}$$

with

$$u(-1/2) = u(1/2) = 0. \tag{5}$$

This is the case studied in [4]–[6]. The analysis will not be repeated here. Rather, we note that the bifurcation diagram for this case appears as in Figure 1. Here, the y-axis measures the maximum displacement of the strip. Notice that for the perfectly conducting strip, the bifurcation diagram is essentially that of the mass-spring model.

4 A Circular Domain

In this section we consider the case where the region Ω is a circular disk of radius one which is held fixed along its circumference. The membrane is assumed to be perfectly conducting and we consider only radially

symmetric solutions. Under these assumptions, equations (2)-(3) reduce to

$$\frac{d^2u}{dr^2} + \frac{1}{r}\frac{du}{dr} = \frac{\lambda}{(1+u)^2} \tag{6}$$

$$u(1) = 0 \tag{7}$$

$$\frac{du}{dr}(0) = 0 \tag{8}$$

Next, we note that this problem exhibits a scale invariance that allows us to obtain solutions from a related initial value problem. That is, $u(r)$ is a solution to equations (6)-(8) if and only if

$$u(r) = -1 + \alpha w(\gamma r) \tag{9}$$

where

$$\alpha = \frac{1}{w(\gamma)} \tag{10}$$

$$\frac{\lambda}{\gamma^2\alpha^3} = 1 \tag{11}$$

and w satisfies the initial value problem

$$\frac{d^2w}{dr^2} + \frac{1}{r}\frac{dw}{dr} = \frac{1}{w^2} \tag{12}$$

$$w(0) = 1 \tag{13}$$

$$\frac{dw}{dr}(0) = 0. \tag{14}$$

With these identifications, the bifurcation diagram is parameterized in terms of γ and w. That is, to understand solutions, we wish to plot λ versus $||u||_\infty = -u(0)$. But from equations (9)-(11) we have $\lambda = \frac{\gamma^2}{w(\gamma)^3}$ and $||u||_\infty = 1 - \frac{1}{w(\gamma)}$. Now, it is a simple matter to sketch the bifurcation diagram for this system. One simply needs to solve equations (12)-(14) numerically or utilize phase plane techniques to analyze the initial value problem completely. Both approaches are carried out in [11]. Here, we note that the bifurcation diagram for this model appears as in Figure 3. Notice that for a given value of the applied voltage, any number of solutions may exist! This is in stark contrast to the system above where a maximum of two solutions were uncovered.

5 A Strip with Varying Dielectric Properties

In this section we again consider the case where Ω is a rectangular strip with two opposite edges fixed and the remaining two edges free. The displacement may be assumed a function of x only. Here however, we do not assume that the strip is perfectly conducting. Rather, we assume that it is a dielectric material and that its dielectric properties vary with position. Under these assumptions, equations (2)-(3) reduce to

$$\frac{d^2u}{dx^2} = \frac{\lambda f(x)}{(1+u)^2} \tag{15}$$

$$u(-1/2) = u(1/2) = 0 \tag{16}$$

If we assume a power law profile for the dielectric properties, $f(x) = |x|^\alpha$, the analysis can be pushed further. This choice of profile is physically motivated as it minimizes the electric field near the region of maximum deflection, hence should tend to stabilize the device. With this choice of profile, our system once again exhibits a scale invariance and can be analyzed by converting to an initial value problem. This is accomplished by setting

$$aw(\eta) = 1 + u(x) \tag{17}$$

$$\eta = bx \tag{18}$$

$$a = \frac{1}{w(b/2)} \tag{19}$$

and

$$\lambda = \frac{b^{2+\alpha}}{w(b/2)^3}. \tag{20}$$

Here, w satisfies the initial value problem

$$\frac{d^2w}{d\eta^2} = \frac{\eta^\alpha}{w^2} \tag{21}$$

$$w(0) = 1 \tag{22}$$

$$\frac{dw}{d\eta}(0) = 0. \tag{23}$$

The bifurcation diagram again follows from analysis of this initial value problem. The reader is directed to [12] for further details. Here, we note that for $\alpha < -\frac{1}{2} + \frac{1}{2}\sqrt{\frac{27}{2}}$ the bifurcation diagram appears as in Figure 1, while for $\alpha > -\frac{1}{2} + \frac{1}{2}\sqrt{\frac{27}{2}}$ the bifurcation diagram appears as in Figure 3. Notice that the system undergoes a transition from a maximum of two solutions to infinitely many steady state solutions.

6 Discussion

We have presented a mathematical model of an idealized small aspect ratio electrostatically actuated membrane type MEMS device. Utilizing the small aspect ratio assumption our problem was reduced to the study of the semi-linear elliptic problem, (2)-(3). While the effect of fringing fields has been ignored, the effects of varying material properties and varying electrode placement have been retained.

We summarized the results of the analysis of our model for three simplified cases. First, we considered a perfectly conducting elastic strip. In this case it is seen

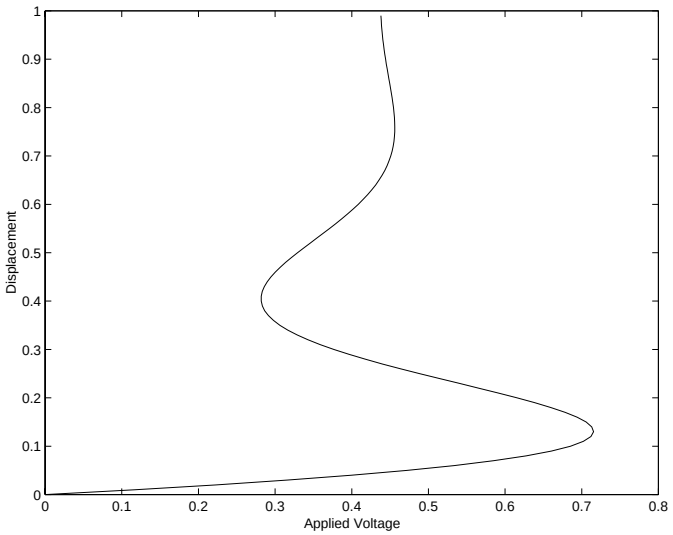

Figure 3: Sketch of the bifurcation diagram for a disk shaped electrostatically actuated MEMS device or a device with varying dielectric properties. Note that the multiple solutions are exaggerated for clarity. Further note that the curve keeps oscillating, producing infinitely many solutions as the displacement tends to one.

that the bifurcation diagram coincides with the diagram most often presented in the literature. That is, the behavior is essentially the same as that for the mass-spring based model introduced in [1]. Next, we considered the case of a perfectly conducting elastic *disk*. In this case, the bifurcation diagram differs dramatically from that of the strip or the mass-spring model. Here, for certain values of the applied voltage, any number of steady state solutions are possible. This simple analysis reveals that *shape* plays an important role in determining device behavior. It suggests that for other device shapes many other behaviors are possible. Finally, we again considered the case of an elastic strip, this time with spatially varying dielectric properties. In this case, according as how the dielectric properties are tailored, the bifurcation diagram may resemble that of the mass-spring model or of the disk model. This analysis reveals that spatial tailoring of the dielectric properties of a device may be used to tailor device behavior. Since varying electrode placement leads to a similar mathematical model, the conclusion holds for electrode design as well. Further, since both mass-spring-like and disk-like behavior can be produced, this suggests that by spatially varying the dielectric properties of a device a wide range of behaviors are possible.

Finally, we comment on the question of stability of solutions. The analysis presented here has been concerned with steady state solutions. A natural question is whether or not the new solutions uncovered are linearly stable or unstable. In fact, a straightforward linear stability analysis reveals that for both the disk and the dielectric strip, all the new solutions uncovered are linearly unstable. On the one hand, this prevents straightforward utilization of these solutions in MEMS design. On the other hand, the opportunity to utilize these new solutions via control schemes presents itself. That is, standard techniques which stabilize near an unstable solution may be useful for some designs. Further, the model, equations (2)-(3), has been analyzed in only the simplest of cases. The possibility of a shaped or electrically tailored device with new *stable* solutions is tantalizing.

7 Acknowledgement

This research was supported by the National Science Foundation under NSF #0071474.

REFERENCES

[1] H.C. Nathanson, R.A. Wickstrom and J.R. Davis, IEEE Trans. on Electron Devices, 14, pp. 117-133, 1967.

[2] P.B. Chu and K.S.J. Pister, Proc. IEEE Int. Conf. Robotics and Automation, pp. 820-825, 1994.

[3] F. Shi, P. Ramesh and S. Mukherjee, Computers and Structures, 56, pp. 769-783, 1995.

[4] D. Bernstein, P. Guidotti and J.A. Pelesko, Proceedings of MSM 2000, pp. 489-492, 2000.

[5] J.A. Pelesko and A.A. Triolo, Proceedings of MSM 2000, pp. 509-512, 2000.

[6] J.A. Pelesko and A.A. Triolo, Jrnl. of Eng. Math., in press, 2001.

[7] J.M. Funk, J.G. Korvink, J. Buhler, M. Bachtold and H. Baltes, J MEMS, 6, pp. 70-82, 1997.

[8] N.R. Aluru and J. White, Proc. of Solid State Sensor and Actuator Workshop, pp. 54-57, 1996.

[9] R. Apte, F. Sandejas, W. Banyai and D. Bloom, Proc. of Solid State Sensor and Actuator Workshop, 1994.

[10] M. Bao and W. Wang, Sensors and Actuators A, 56, pp. 135-141, 1996.

[11] J.A. Pelesko and X.Y. Chen, J. MEMS, submitted. (email: pelesko@math.gatech.edu for preprint)

[12] J.A. Pelesko, SIAM Jrnl. Appl. Math, submitted. (email: pelesko@math.gatech.edu for preprint)